Hindawi
Advances in Civil Engineering
Volume 2023, Article ID 6692079, 10 pages
https://doi.org/10.1155/2023/6692079

Research Article

Pressure-Shear Crack Initiation and Expansion Mechanism of Complex Cracked Rock Mass under the Seepage Stress

Lu Shen

Wanjiang University of Technology, Maanshan 243011, China

Correspondence should be addressed to Lu Shen; 156051459@qq.com

Received 21 February 2023; Revised 21 April 2023; Accepted 14 November 2023; Published 7 December 2023

Academic Editor: Tayfun Dede

This work was to analyze and discuss the propagation mechanism of compressive shear initiation of complex fractured rock mass with seepage stress. The dense marble of Daye Iron mine with bulk density of 26.6 kN/m^3 and uniaxial compressive strength of 52.4 MPa was selected as the material, and the upper and lower fracture surfaces were polished smoothly. The crack initiation criterion under compressive shear stress state is analyzed by taking the theory of fracture mechanics and classical mechanics. The coupling equation in the extended finite element simulation is established. The influence of lateral pressure on the crack propagation law, the relationship between lateral pressure and fracture, the initial expansion angle and pressure change law, and the effect of working face length on the crack expansion are analyzed. *Results.* The initial expansion angle of cracks increases with the increase of lateral pressure, and that of a single crack decreases with the increase of pressure. When other conditions are constant, the crack angle of the crevice also shows a trend of increasing with the increase of lateral pressure. When the lateral pressure becomes smaller, the initial expansion angle is relatively small. With the progress of the step size, the expansion angle shows a gradually decreasing trend, that is, the initial expansion angle gradually decreases with the increase of water pressure. The smaller the working face length, the smaller the expansion length of the floor crack. *Conclusion*. The expansion of the floor cracks is mainly formed by the tensile shear failure, and the fracture water pressure will reduce the initiation stress, which makes the rock mass more prone to the fracture failure.

1. Introduction

In recent years, with the rapid development of the national economy, the related problems under the action of engineering rock mass seepage and stress have become a problem faced by many scholars in engineering disciplines. More than 90% of rock slopes are related to the infiltration of low water, and the dynamic equilibrium system under the action of rock seepage and stress has become a topic worthy of attention in the field of rock mechanics [1–3]. Cracks or the expansion of cracks can cause damage to the cracked rock mass. Underground water not only affects rock mechanics but also rock mass mechanics. Rock mass is a variable factor in mechanics, and the result of its effect in mechanics is not very clear. Many mine accidents are related to low water, and the infiltration of rock mass is also a very important reason for the failure of 30%–40% of hydropower projects [4]. Therefore, the coupling effect between seepage and stress in rock mass should be worthy of attention.

A very important subject in the field of rock mechanics is the change of the stability mechanism between the seepage and stress of fractured rock mass. Human engineering activities cannot avoid the transformation of adverse geological environment. In order to have a better living ecological environment, the excavation of the project is basically based on the change of the stress field in the rock body, which will inevitably lead to changes in the regional or local underground water discharge environment of the rock mass. After the artificial disturbance of the low-water seepage field, the mechanical action strength and action form of the rock mass will change to a certain extent, and these uncertain changes will affect the stability of the fractured rock mass [5]. Fractured rock mass contains many macroscopic discontinuities, mainly including voids, microcracks, defects, and joints. The distribution of stress field changes due to underground

water, resulting in crack expansion. This interaction between them is called seepage–stress coupling [6]. The failure of the Malpasset arch dam in France in 1959 was a typical example of seepage–stress coupling, and people gradually realized the importance of fractured rock mass to engineering safety [7]. It is necessary to study the activity law of underground water in rock mass and the mechanism of seepage–stress coupling [8]. With the continuous expansion of the project scale, the geotechnical engineering community is particularly urgent to solve this problem.

A large number of voids and cracks in natural rock mass affect the mechanical properties of rock mass. There is anisotropy between the rock masses, the strength parameters are reduced, and the permeability characteristics of the rock mass are also affected [9]. The characteristics of rock mass seepage include unsaturated seepage, seepage anisotropy, and seepage inhomogeneity. In different directions, the rock permeability characteristics show differences, showing the anisotropy of rock mass seepage, which is generally expressed by the permeability tensor. The main factors that produce seepage anisotropy are: inhomogeneity of spatial distribution and grouping of discontinuous surfaces [10]. The permeability of the rock mass shows a certain dominance in the direction where the joints and cracks are dense [11]. Due to the difference in opening and roughness between discontinuous surfaces, the seepage characteristics are also quite different. The place with a large opening becomes the dominant seepage channel, while for some gas-sealed areas; the seepage diameter is more complicated. Some exploration shows that although some cracks are below the underground water level, they are still dry or have only a small amount of crack water seepage, which shows the unsaturated state of the rock mass [12, 13]. The inhomogeneity of seepage is mainly reflected in the different permeability coefficients at different positions in the rock mass space system. The spatial function of coordinates is the permeability coefficient. The reason for the inhomogeneity is the different distribution of pores and joints [14, 15]. There is a crack in the rock mass, and the water pressure expansion causes the intensification of the expansion process of the rock mass, which in turn causes the macroscopic damage of the cracked rock mass and the reduction of the strength of the rock mass. The expansion of crack changes the characteristics of seepage, the distribution of seepage field changes, and there is a coupling effect between seepage and damage of rock mass [16, 17].

The use of fracture mechanics theory to study the failure mechanism of crack rock mass began in the 1960s, and has become a new branch of rock mechanics in the past 10 years. The research directions of the scholars mainly include rock fracture toughness test, crack expansion law, and tensile–shear and compression–shear coincidence fracture [18, 19]. The coupling interaction between seepage field and stress field is mainly to study the basic law of interaction between solid and tumor medium. Vandalnlne and Roegiers [20] has proposed a coupled solution for hydraulic fracturing. Liu et al. [21] used the stress–seepage damage coupling model to discuss the pore pressure during excavation. With the increase of construction time, the pore pressure first increased and then decreased. However, the sparseness of the damaged area and the infiltration area gradually increased. Liu et al. [22] explored the crack interaction mechanism of crack media with irregular geometric parameters under uniaxial and biaxial compression conditions. The parameter controlling the failure mode of the specimen includes the crack length. The seepage–stress coupling gradually attracted the attention of theoretical experts, and a large number of experimental studies and a large number of data came into being [23]. However, due to the complexity of the seepage stress of the rock mass fusion, there are many uncertain factors in the discussion of this issue, and theoretical research and experimental research are still in an immature stage. The cracks of different sizes and different orientations in the rock mass make it impossible for each crack to determine the specific geometric parameters of the crack. For these randomly distributed media, only the seepage theory can not well reflect the expansion of aggregate cracks and new city cracks in the seepage coupling process. Therefore, it is necessary to continue to explore the coupling of seepage and stress field in the cracked rock mass to provide more reference for future engineering implementation and application.

At present, the permeability mechanism of fractured rock mass is not clear. The innovations of this study lie in three aspects. First, the rock mass fracture mechanics are introduced to the analysis of fractured rock mass based on the theory of fracture mechanics. Second, the influence of stress and strain on the permeability coefficient of fractured rock mass is analyzed by using mathematical model. Third, the coupling changes of seepage field and stress field in the fractured rock mass are investigated from the angle of pressure shear crack, which can provide reference for the theoretical application.

2. Materials and Methods

2.1. Coupling Analysis of Seepage and Stress in Crack. The mechanical properties of the cracked rock mass will be affected to a certain extent by the existence of underground water. The seepage force applied to the cracked rock mass will reduce its strength, which directly affects the temperature and deformation of the rock mass. Deformation and stability analysis of joint crack rock mass is very important for seepage imaging. Seepage has strong stress and deformation dependence. After the cracked rock mass is loaded, the stress field changes gradually, the normal and tangential stresses of the crack gradually increase, the voids in the rock mass and the crack opening degree change, and the seepage channel of the rock mass also changes. On the other hand, the seepage pressure generated by seepage reduces the effective normal stress on the crack surface of the joint, and the stability and deformation of the rock mass will be reduced. The relationship between the stress of cracked rock mass and the seepage coefficient is shown in Figure 1. After the rock mass is loaded, the change of the stress field force causes the change of the opening degree of the rock mass and the crack, the flow velocity of the seepage and the pressure redistribution of the fluid in the table, and the water

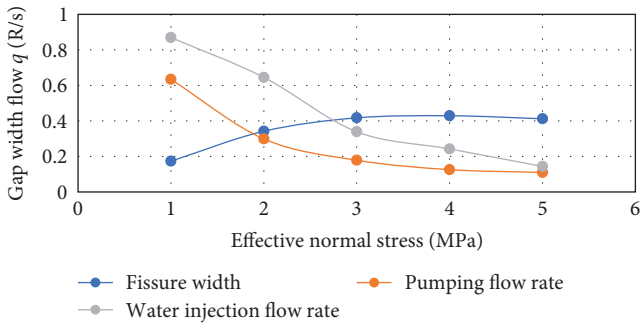

Figure 1: The relationship between crack opening and water flow and effective normal stress.

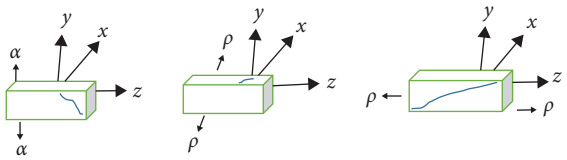

Figure 2: Schematic diagram of crack types.

flux in the crack decreases with the increase of normal stress of the crack.

2.2. Fracture Model of Seepage Stress Coupling. After the action of various stresses such as tension, compression, and torsion, the structural characteristics of the cracked rock mass will remain after countless transformations, and there is still a certain regularity.

The fracture modes of rock mass cracks mainly include three types of cracks as shown in Figure 2, namely, Type I cracks, Type II cracks, and Type III cracks. Type I cracks become open, and the displacement of the crack surface is perpendicular to the crack surface. Type II cracks are also called slip shear. Type III cracks have discontinuities in the Z direction of the upper and lower surface points on the surface, and are also called tearing or shearing.

According to the theory of fracture mechanics and classical mechanics, a coupled seepage–stress model is established. Figure 3(a) shows a single crack in tension, and Figure 3(b) is a schematic diagram of a single pure shear crack. Figure 3(c) is an equivalent schematic diagram of a single pure shear crack. The stress concentration occurs at the crack tip under tension at the maximum position of the crack. When KI ≥ KIC, the shear effect will appear, and the crack plane will gradually expand outward. Figure 3(b) shows the path of the crack expansion. The state of the crack subjected to pure shear stress is shown in Figure 3(b). Figure 3(b) is equivalent to Figure 3(c), then $\alpha 1 = \alpha 2 = /2\text{ϒ}$. When KI ≥ KIC crack initiation, the initiation angle is 70.5°. The expansion direction is shown in Figure 3.

The maximum circumferential stress theory contains two basic assumptions: the first is that the crack expansion occurs when the maximum circumferential stress reaches the critical stress, and the second is that the crack will expand in the direction of the maximum circumferential stress value. The critical stress condition can be determined according to

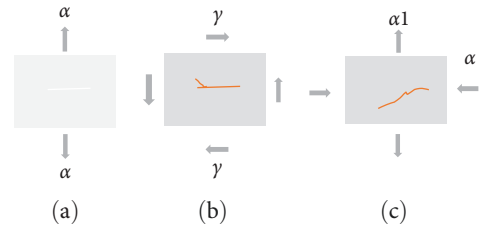

Figure 3: Equivalent schematic diagram of hand fracture with different cracks ((a)–(c)).

the first basic assumption, and the crack initiation angle can be derived from the second basic assumption. The stress components at the crack tip of Type I and Type II are superimposed, and the polar coordinate stress component Equations (1)–(3) at the crack tip are expressed as follows:

$$\alpha_\rho = \frac{1}{2\sqrt{2\pi\rho}}\left[K1\left(3-\cos\frac{\theta}{2}\right)\right] + KII(3\cos\theta - 1)\sin\frac{\theta}{2}, \tag{1}$$

$$\alpha_\theta = \frac{1}{2\sqrt{2\pi\rho}}\cos\frac{\theta}{2}\left[K_1\cos^2\frac{\theta}{2} - \frac{3}{2}\mathrm{K_{II}}\sin\theta\right], \tag{2}$$

$$\gamma_{\rho\theta} = \frac{1}{2\sqrt{2\pi\rho}}\cos\frac{\theta}{2}[K_1(\sin\theta) + KII(3\cos\theta - 1)]. \tag{3}$$

In the equation, Θ is the crack initiation angle, α refers to the axial stress, and the circumferential stress $\alpha\Theta$ takes the extreme value to obtain the crack initiation angle Θ, the equation is as follows:

$$\frac{\partial\alpha_\theta}{\partial\theta} = 0. \tag{4}$$

It should continue to take the derivative of Θ for the second time, and the equation is expressed as follows:

$$\frac{\partial\alpha_\theta}{\partial\theta} = \frac{-3}{4\sqrt{2\pi\rho}}\cos\frac{\theta}{2}[K_1\sin\theta + K_{II}(3\cos\theta - 1]. \tag{5}$$

According to the equation, the crack expansion angle Θ_0 is obtained, and the calculation equation is as follows:

$$\theta_\theta = \begin{cases} 2\mathrm{arctg}\left[|K_1| - \sqrt{{K_1}^2 + 8{K_{II}}^2}\right] K_{II} \neq 0 \\ 0 K_{II} = 0 \end{cases}, \tag{6}$$

$$\rho = \rho_0. \tag{7}$$

The equation for the maximum circumferential stress on the circumference is expressed as follows:

$$\alpha_{\theta\max} = \frac{1}{2\sqrt{2\pi\rho_0}} \cos\frac{\theta_0}{2}\left[K_1(1+\cos\theta_0) - 3K_{II}\sin\theta_0\right]. \tag{8}$$

According to the second assumption of maximum circumferential stress, the fracture criterion is expressed by the equation as follows:

$$\alpha_{\theta\max} = \alpha_{\theta c}. \tag{9}$$

The critical value stress of $\alpha\Theta$c can be determined according to the fracture toughness KIC of the first type of crack. The expansion of the first type of crack is always along the crack surface. Therefore, the cracking angle can be taken into the equation as follows:

$$\theta_0 = 0, K_{II} = 0,\ K_I = K_{IC}. \tag{10}$$

The critical value for obtaining the maximum circumferential stress is expressed as Equation (11) below:

$$\alpha_{\theta c} = \frac{K_{IC}}{2\sqrt{2\pi\rho}}. \tag{11}$$

After Equation (11) and Equation (8) are incorporated into Equation (9), the below equation can be obtained as follows:

$$K_{\mathrm{IC}} = \frac{1}{2}\cos\frac{\theta_0}{2}\left[K_1(1+\cos\theta_0) - 3K_{II}\sin\theta_0\right]. \tag{12}$$

This is the basis for judging the cracks of the first type and the second type of composite type.

For a Type I crack, which is incorporated into the Equation (12), then, the following expression can be obtained:

$$\cos\theta_0 \frac{1}{3}. \tag{13}$$

2.3. Crack Expansion Length. The schematic diagram of the crack force of the two cracks in the geese, the schematic diagram of the expansion of the branch crack, and the force of the crack tip. F represents the water pressure; $\alpha 1$ and $\alpha 2$ represent the principal stress in the crack, and the direction is perpendicular to the crack surface. The theory of elasticity is adopted, and the equations of the normal stress (ζ) and shear stress (α) on the crack surface are given as follows:

$$\zeta = \frac{\alpha 1 - \alpha 3}{2}\sin 2\beta, \tag{14}$$

$$\alpha = \frac{\alpha_1 + \alpha_3}{2} + \frac{\alpha_1 - \alpha_3}{2}\cos 2\beta. \tag{15}$$

The crack surface is subjected to compressive shear load, and the resulting slip force is expressed as below equation:

$$F_{\mathrm{s}} = \zeta + f(\alpha + P). \tag{16}$$

F_{s} is the tangential force on the branch crack, and Fn is the normal force on the branch crack. P represents water pressure.

The tangential stress $\alpha_{\Theta\Theta}$ at the tip at an angle to the original crack determined by the driving sliding force is expressed as follows:

$$\alpha_{\theta\theta} = \frac{3Fs\sqrt{\pi\alpha}}{2\sqrt{2\pi\rho}}\sin\theta\cos\frac{\theta}{2}. \tag{17}$$

The expression factor of stress intensity factor at a tiny crack m at the crack tip is expressed as follows:

$$K_I = \frac{3}{2}Fs\sqrt{\pi}\sin\theta\cos\frac{\theta}{2}. \tag{18}$$

When the crack is sheared, the extreme value is obtained according to the effective shear stress, and the expression equation is as follows:

$$\frac{\partial Fs}{\partial\phi} = 0, \tag{19}$$

$$\frac{\partial^2 Fs}{\partial^2\phi} < 0. \tag{20}$$

Then, the equation for the brute force factor is expressed as follows:

$$K_I = \left(\frac{\pi\alpha}{3}\right)^{\frac{1}{2}}[\alpha_3 - \alpha_3]\sqrt{1+\mathrm{f}^2\pi} + \mathrm{f}(\alpha_1 + \alpha_3). \tag{21}$$

When the external forces $\alpha 1$ and $\alpha 2$ reach a certain value, the twill surface will slide; forming a branch crack at the crack tip, and the crack expansion direction is parallel to the direction of the maximum compressive stress.

2.4. Finite Element Analysis of Crack Expansion with Seepage Stress Coupling. The research on rock mass includes theoretical research, numerical simulation, and experimental research, and the theoretical solution of simple problems can be obtained by using theoretical research. However, it can not deal with particularly complex problems. Numerical simulation can accurately carry out numerical simulation analysis of crack expansion of the crack rock mass, and can achieve rapid development. The method of experimental research is relatively inconvenient in practical application, but it can directly form the expansion law for simulating crack. Experiment is the spine of numerical simulation, and numerical simulation is the in-depth discussion of experimental research. The combination of these two methods can handle many problems well. The in-depth study of rock mass failure mainly relies on the synergistic analysis of these three methods. In this work, the expansion study in the seepage coupling process in crack is analyzed,

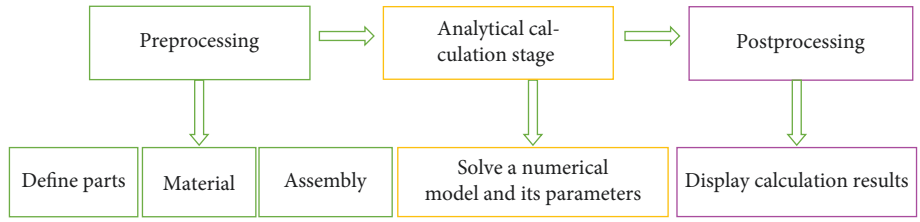

Figure 4: Schematic diagram of expansion finite element analysis flow.

and the expansion law of cracked rock mass under different water pressures is discussed.

Expansion finite element is to use discontinuous shape function to express the regional discontinuity in the calculation area. The mesh boundary in the calculation process has no relationship with the description of the discontinuous field, and it shows superiority when dealing with fractures. Any path in crack expansion can be simulated concisely and comprehensively using the finite element method of expansion. First, the expansion finite element numerical simulation software ABAQUS is used to analyze the simple linear analysis and the complex flying linear problem to simulate the performance of typical engineering materials. Numerical simulation research can also solve many problems in the field of engineering geology by noduling the problems of stress and strain. The steps of the analysis flow of expansion finite element are shown in Figure 4. It should preprocess some physical models such as defined parts, materials, and assemblies to generate a file, solve the numerical model and its parameters defined in the input file, and then read the result data. The ways of presenting the results include expansion diagrams, animations, cloud diagrams, and deformation diagrams.

2.5. Establishment of Coupling Equations in Expansion Finite Element Simulation. The fluid–solid coupling theory is widely used in the processing of petroleum, harmful nuclear waste, and earthquakes in reservoirs, and it has also become a newly emerging subject of the interaction between fluid and rock mass. On the basis of elastic mechanics, the stress balance equation is expressed by the principle of virtual work. In the equation, the virtual work of the rock mass and the virtual work generated by the external force are equal, and the expression equation is as follows:

$$\int_V \delta\varepsilon^T \mathrm{d}\sigma \mathrm{dV} - \int_V \delta u^T \mathrm{d}f \mathrm{dV} - \int_V \delta u^T \mathrm{dtdS} = 0. \tag{22}$$

In the equation above, T represents the surface force, f represents the body force, $\delta\varepsilon$ represents the virtual stress, and δu represents the virtual displacement.

The constitutive relation can be expressed in incremental form as follows:

$$\mathrm{d}\sigma = \mathrm{W}_{\mathrm{ep}}(d\varepsilon - d\varepsilon_1). \tag{23}$$

$d\varepsilon_1$ refers to the particle compression, as expressed in Equation (24), and W_{ep} is the elastoplastic matrix.

$$d\varepsilon_1 = -m\frac{d\overline{p}}{3K_s}. \tag{24}$$

In the above equation, $m = [1, 1, 1, 0, 0, 0]^T$

The effective stress expression is shown as follows:

$$\sigma = \sigma + \alpha\, \mathrm{m}\overline{p}. \tag{25}$$

$\overline{p}$ represents the average pressure of the two fluids:

If $\alpha = 1$, Equation (26) can be obtained from Equations (22), (23), and (25) as follows:

$$\int_V \delta\varepsilon^T W_{\mathrm{ep}}\left(d\varepsilon_1 + m\frac{d\overline{p}}{3K_s}\right)\mathrm{dV} - \int_V \delta\varepsilon^T \mathrm{m}\mathrm{d}\overline{\mathrm{p}}\mathrm{dV} - \int_V \delta u^T \mathrm{dfdV} - S = 0. \tag{26}$$

If the pressure is constant, then the equation below could be obtained as follows:

$$\frac{d\mathrm{p}_a}{d_t} = 0. \tag{27}$$

Therefore, the derivative of the mean void pressure with respect to time can be simplified as Equation (28):

$$\frac{d\overline{p}}{\mathrm{d}t} = \frac{d(s_w p_w + (1 - s_w)p_a)}{dt} = s_w\frac{d_w}{\mathrm{d}t} + p_w\frac{ds_w}{\mathrm{d}t}. \tag{28}$$

S_w is saturation, P_w is void pressure, and P_a is void air pressure, with $P_a = 0.1$ MPa, which is a standard atmospheric pressure. S_w is a function of void water pressure, as expressed in Equation (29):

$$\frac{ds_{\mathrm{w}}}{\mathrm{d}t} = \frac{ds_w}{dp_w}\frac{d_w P_w}{\mathrm{d}t} = \psi\frac{dp_w}{\mathrm{d}t}, \tag{29}$$

where ψ represents the capillary pressure, which is determined by the saturation test, so Equation (30) below can be obtained as follows:

$$\frac{d\overline{p}}{\mathrm{d}t} = (s_w + p_w\psi)\frac{dp_w}{\mathrm{d}t}. \tag{30}$$

Equation (31) is obtained by combining the Equations (26) and (30) as follows:

$$\int_V \delta\varepsilon^T W_{\mathrm{ep}}\left(\frac{d\varepsilon}{\mathrm{d}_t}\right)\mathrm{dV} + \int_V \delta\varepsilon^T W_{\mathrm{ep}}\left(m\frac{(s_w + p_w\psi)}{3K_s}\frac{dp_w}{\mathrm{d}t}\right)\mathrm{dV} - \int_V \delta\varepsilon^T \mathrm{m}(s_w + p_w\psi)\frac{dp_w}{dt}\mathrm{dV} = \int_V \delta u^T \frac{df}{dt}\mathrm{dV} + \int_V \delta u^T \frac{dt}{dt}\mathrm{dS}. \tag{31}$$

The seepage field contains two boundary conditions: one is the flow boundary condition, and the other is the pore pressure boundary condition. The flow boundary condition is expressed as follows:

$$-\mathrm{e}^T K K_r\left(\frac{P_w}{\rho_w} - g\right) = q_w. \tag{32}$$

In the above equation, e represents the unit normal vector of the boundary surface, and q_w is the flow rate of water flowing through the flow boundary.

The pore pressure boundary conditions satisfy the following equation:

$$P_w = P_{wb}. \tag{33}$$

2.6. Experimental Methods. Coal seam floor water inrush is a complex geological phenomenon, which is affected by the factors such as mining pressure, water pressure of confined water in aquifers, lithologic characteristics of aquifers in coal seam floor, and water-rich aquifers. In order to calculate the limit water pressure value of the impedance water of the bottom plate, a mechanical model of the bottom plate is established, and the length of the working face is L. Figure 5 shows the numerical calculation model of the base plate.

The physical parameters of the rock mass are shown in Table 1.

The relationship between permeability coefficient and shear stress is discussed, and the conditions of low stress and low-water head are selected. In the test, a vertical Qianjin top is selected to apply normal pressure to the crack surface, a vertical dial gauge is used to record the corresponding dial gauge value and flow rate, and the seepage flow under the corresponding shear stress is measured. The record of seepage flow is measured indirectly. The test measures the time it takes for three water flows to fill a measuring cup of a certain volume, and the average value is taken during the calculation process.

3. Results

3.1. Influence of Lateral Pressure on Fracture Expansion Law. Lateral pressure plays a very important role in crack initiation, expansion, and penetration. Under the condition that the physical parameters remain unchanged, a crack inclination model (45°, 60°) is established to simulate the influence of water pressure on crack initiation and expansion. The lateral pressures are 0.1, 0.2, 0.3, and 0.4 MPa, respectively. Figure 6 suggests that the water pressure shows an increasing trend with the increase of the time step. The larger the inclination angle, the greater the water pressure.

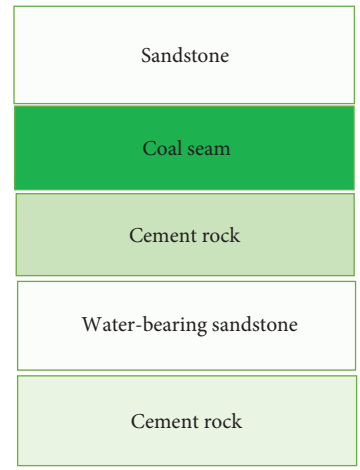

Figure 5: Numerical calculation model of the base plate.

3.2. Analysis of the Relationship between Lateral Pressure and Fracture. When other conditions are constant, with the increase of lateral pressure, the crack angle also tends to increase; when the lateral pressure becomes smaller, the initial expansion angle is also relatively small, which shows that the splitting effect of water pressure on the rock mass is more obvious. The expansion angle becomes larger, the lateral pressure becomes larger, the crack tends to expand in the vertical direction, and the splitting effect of the water pressure decreases. Figure 7 shows the results of the initial expansion angle under different pressures with a crack inclination angle of 45°. When the lateral pressures are 0.1, 0.2, 0.3, and 0.4 MPa, respectively, and the expansion angles are 40°, 50°, 52°, and 68°, respectively.

Figure 8 shows the results of initial expansion angles under different pressures with a crack inclination angle of 60°. When the lateral pressures are 0.1, 0.2, 0.3, and 0.4 MPa, respectively, and the expansion angles are 42°, 53°, 56°, and 67°, respectively. The schematic diagram of the initial expansion angle of the two angles with the pressure is shown in Figure 9, and the expansion angle shows an increasing trend with the increase of the pressure.

3.3. Effect of Water Pressure on Fracture Expansion. Water pressure has a relatively complex change in the mechanical properties of rock mass. After the lateral pressure is constant, the physical parameters and other loading conditions remain unchanged, and the influence of the water pressure on the crack expansion of the 45° and 60° models is analyzed. As shown in Figure 10, under different water pressures of 0.1, 0.2, 0.3, and 0.4 MPa, the water pressure at the midpoint gradually increased and finally showed a stable trend with the progress of the step.

Table 1: The physical parameters of the rock mass.

	Sandstone	Coal seam	Cement rock	Water-bearing sandstone	Cement rock
Thickness m	20	3	30	40	65
Elastic modulus (GPa)	2.6	16	18	36	18
Compressive strength (MPa)	60	25	40	90	35
Poisson's ratio	0.2	0.32	0.25	0.15	0.27
Permeability coefficient (m/d)	0.01	0.01	0.01	100	0.01
Homogeneity	5	10	2	4	2

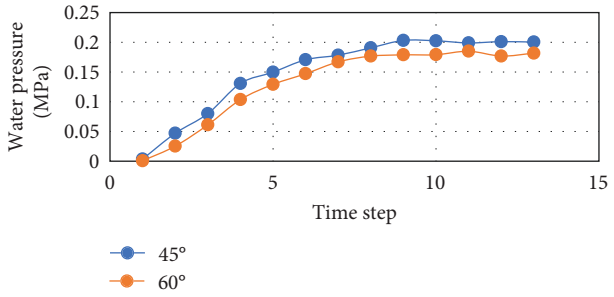

Figure 6: Change of water pressure at the midpoint of the model point sample with time step.

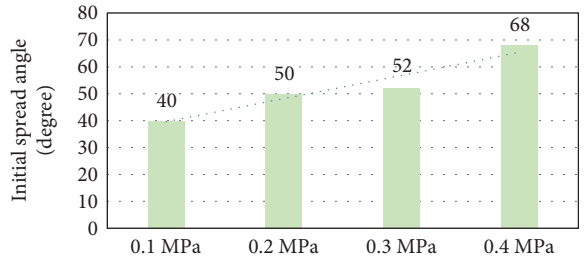

Figure 7: Fracture dip angle of 45° initial expansion angle under different lateral pressures.

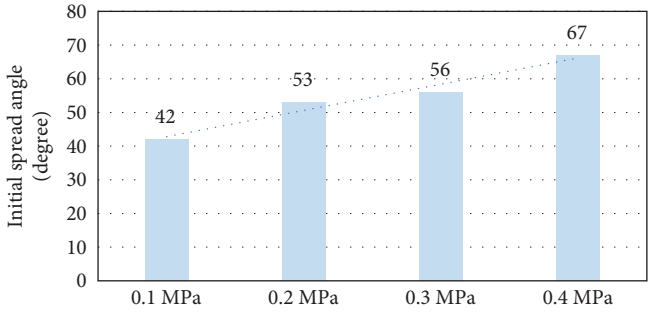

Figure 8: The initial expansion angle under different lateral pressures with fracture dip angle of 60°.

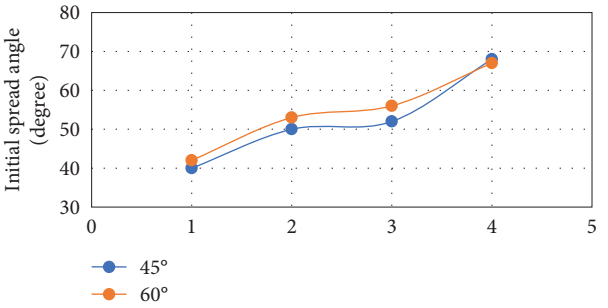

Figure 9: Variation of expansion angle with pressure.

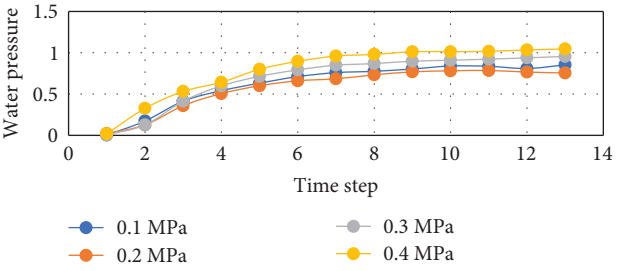

Figure 10: Variation of different water pressures with step.

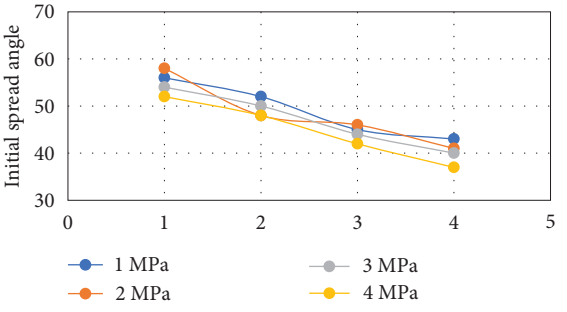

Figure 11: Trend of expansion angle versus pressure.

3.4. Initial Expansion Angle and Pressure Variation Law. For a single crack, after the lateral pressure is constant and other loading conditions and physical parameters remain unchanged, the influence of different water pressures on the expansion angle of the crack is analyzed. As shown in Figure 11, under different water pressures of 0.1, 0.2, 0.3, and 0.4 MPa, the expansion angle shows a gradually decreasing trend, that is with the progress of the step, which means that the initial expansion angle gradually decreases as the water pressure increase.

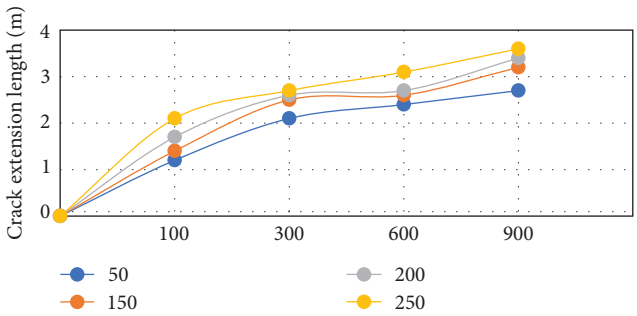

Figure 12: Effect of working face length on floor crack expansion.

3.5. Effect of Working Face Length on Gap Expansion. The floor expansion is driven by the Eurasian shear stress, and as the mining progresses, the fractures expand gradually. As shown in Figure 12, when the thickness of the water barrier and the mechanical properties of the rock mass are kept constant, the length of the working face increases, which leads to an increase in the length of the crack expansion, which reduces the ability of the floor to resist water. That is to say, the smaller the length of the overall working face, the larger the water pressure value of the bottom water inrush limit becomes.

4. Discussion

Underground water has a certain influence on rock mechanics and mechanical properties of rocks. After the rock mass in the crack is subjected to the force, it will deform. As a bridge between the seepage field and the stress field, the permeability coefficient connects the coupling relationship between the two, and it also changes with the change of crack under the action of force. After the coupling relationship is generated, the phenomenon of seepage–stress coupling of crack rock mass can be better understood [24]. Many scholars have carried out research on the coupling of rock mass seepage, and some people have proposed the idea of static inversion of even coupling parameters, which is also a hot spot in this field. On the basis of traditional parameter inversion, a fully coupled analysis is carried out on various types of observational data such as head and displacement. It also provides a powerful tool for some uncertain parameters. The construction of rock mass engineering and the environment are constantly changing over time. The observation of rock mass seepage and mechanical behavior also needs to be deepened [25, 26]. There are many changing factors that need to be considered for the seepage and stress of cracked rock mass. This kind of research is also a relatively complex topic, and it is necessary to comprehensively consider many aspects such as dynamics and rock mass structure. The natural geological body of the rock mass itself constitutes a highly complex and uncertain system, and people's understanding of it is still uncertain, and there are still many problems to be solved. At this stage, many scholars have carried out a lot of research on the positive aspect of seepage. Pang et al. [27] independently designed a triaxial seepage system in order to study the recrushing mechanism and seepage characteristics of crushed coal medium under load. Using the steady-state infiltration method, various flow factors of the crushed coal medium under different particle size combinations and different stress conditions are obtained. On the one hand, the reduction of the porosity of the crushed coal medium will lead to the reconstruction of the flow channel, and the sudden change of the flow will directly lead to the non-Darcy flow regime. On the other hand, the seepage throat in the crushed coal medium may experience a sharp increase in flow velocity, resulting in abrupt changes in the flow regime. The law obtained according to the seepage characteristics can be used as the calculation basis for the prevention and control of mine water inrush accidents. Shao et al. [28] established a micromechanics-based stress–seepage–damage coupled model to simulate the initiation and expansion of cracks in rock materials and their interaction with fluid flow. The model provides an intuitive understanding of the evolution process of rock failure and water inrush, which is difficult to observe, and helps to prevent water inrush disasters in practical engineering. The influence of surrounding rock pressure on the failure of fractured rock mass is significant. When the confining pressure is low, the failure is brittle. When the confining pressure is high, the rock mass shows the property of soft rock.

It is very important to analyze the effect of lateral pressure on crack propagation to understand the mechanical properties of rock mass. In this study, the law of lateral pressure on crack propagation was analyzed. Under the condition of constant physical parameters, the crack inclination model (45° and 60°) was established to simulate the influence of water pressure on crack initiation and propagation. The water pressure increases with the increase of time step, and the greater the inclination angle, the greater the water pressure. When other conditions are fixed, the crack angle also shows an increasing trend with the increase of lateral pressure. When the lateral pressure changes, the initial expansion angle is relatively small, which indicates that the water outlet pressure has an obvious splitting effect on the rock mass. As the expansion angle increases, the lateral pressure increases, the crack tends to expand in the vertical direction, and the splitting effect of water pressure decreases. When the lateral pressure is small, the initial propagation angle is relatively small, and the wing crack is more inclined to spread in parallel axial direction, which also shows that the water outlet pressure has a more obvious effect on the fracture of rock mass.

In the seepage of crack network rock mass, when the rock mass presents a discontinuous distribution, the seepage mainly depends on the relatively large fracture. If a relatively continuous medium or an equivalent continuous medium is used for processing, a relatively large error will occur. The results of low-water permeability calculated by the discontinuous medium method are almost consistent with the actual results [29]. There are many uncertainties in the rock mass, cracks of different sizes and the expansion of the cracks of the heart. To solve these problems, it is necessary to continuously introduce new theoretical methods. This work explores the crack expansion rule under seepage stress

coupling. The results show that as the lateral pressure increases, the initial expansion angle of the crack also increases, and the initial expansion angle of a single crack decreases with the increase of the pressure. In the change law of initial expansion angle and pressure, the expansion angle of different water pressures gradually decreases with the step length, that is, the initial expansion angle gradually decreases with the increase of water pressure. The limit model of floor resistance to water inrush shows that the smaller the length of working face, the smaller the extension length of floor crack, and the expansion of floor crack is mainly formed in the form of tensile shear failure. When other physical parameters are unchanged, the initial expansion angle of single crack increases with the increase of lateral pressure. When the water pressure is changed, the initial expansion angle of single crack decreases with the increase of water pressure. The geometric characteristics of fracture are closely related to the seepage characteristics of rock mass, and the geometric parameters of fracture will also change when the stress field of rock mass changes, which also indicates that there is a strong coupling effect between the seepage field and the stress field of the fractured rock mass. The study of spectrum sum of fractured rock mass is also a complex subject, and a large number of coupling studies have been carried out by scholars all over the world. However, how to determine the coupling parameters, how to determine the seepage, stress, etc., has been a key problem in the field of rock mass research. There are still many problems to be solved in the mechanism of rock mass press-shear initiation and further work needs to be done.

5. Conclusions

This work aims to explore the crack expansion law under seepage stress coupling. Based on the theory of fracture mechanics and classical mechanics, the crack initiation criterion under compressive shear stress state is analyzed starting from the direction of crack expansion. As the lateral pressure increases, the initial expansion angle of the crack also increases gradually, and the initial expansion angle of a single crack decreases with the increase of the pressure. The water inrush resistance limit model of the floor is used to show that the smaller the working face length is, the smaller the expansion length of the floor crack will be, and the tensile shear failure is the main reason for the expansion of the floor crack. There are many future research directions. What is the expansion law of various cracks? The influence of the factors such as lateral pressure, crack inclination angle, and crack spacing in this process is also a direction worthy of in-depth study. In addition, floor water inrush is also a complex project. What are the factors of floor water inrush? What kind of impact results will be produced? Further exploratory research can also be done to provide more comprehensive theoretical data and provide a reference for the application of rock mass seepage.

Data Availability

The data used to support the findings of this study are available from the corresponding author upon request.

Disclosure

The statements, opinions, and data contained in all publications are solely those of the individual author and contributor(s) and not of MDPI and/or the editor(s). MDPI and/or the editor(s) disclaim responsibility for any injury to people or property resulting from any ideas, methods, instructions, or products referred to in the content.

Conflicts of Interest

The author declares that there is no conflict of interest.

Acknowledgments

“This research received an external funding,” grant number “gxyq2021243” and “The APC was funded by “College Excellent Talents Support Program of Education Department of Anhui Province” grant number “2020 KJ2020A0836” and “the Natural Science Research Project of Universities in Anhui Province of Education Department of Anhui.”

References

[1] J. Liu, S.-L. Chen, H.-J. Wang, Y.-C. Li, and X. Geng, “The migration law of overlay rock and coal in deeply inclined coal seam with fully mechanized top coal caving,” *Journal of Environmental Biology*, vol. 36, no. 4, 2015.

[2] X. Xiong, J. Dai, Y. Ouyang, and P. Shen, “Experimental analysis of control technology and deformation failure mechanism of inclined coal seam roadway using non-contact DIC technique,” *Scientific Reports*, vol. 11, no. 1, Article ID 20930, 2021.

[3] G. Liu, Y. Chen, X. Du, P. Xiao, S. Liao, and R. Azzam, “Investigation of microcrack propagation and energy evolution in brittle rocks based on the voronoi model,” *Materials*, vol. 14, no. 9, Article ID 2108, 2021.

[4] H. Wang, Y. Qin, H. Wang, Y. Chen, and X. Liu, “Process of overburden failure in steeply inclined multi-seam mining: insights from physical modelling,” *Royal Society Open Science*, vol. 8, no. 5, Article ID 210275, 2021.

[5] Y. Li, H. Zhang, M. Chen et al., “Strength criterion of rock mass considering the damage and effect of joint dip angle,” *Scientific Reports*, vol. 12, no. 1, Article ID 2601, 2022.

[6] S. Xu, S. Wang, P. Zhang, D. Yang, and B. Sun, “Study on strain characterization and failure location of rock fracture process using distributed optical fiber under uniaxial compression,” *Sensors*, vol. 20, no. 14, Article ID 3853, 2020.

[7] G.-S. Wu, W.-J. Yu, J.-P. Zuo, C.-Y. Li, J.-H. Li, and S.-H. Du, “Experimental investigation on rockburst behavior of the rock–coal–bolt specimen under different stress conditions,” *Scientific Reports*, vol. 10, no. 1, Article ID 7556, 2020.

[8] A. M. Shapiro, C. R. Tiedeman, T. E. Imbrigiotta et al., “Bioremediation in fractured rock: 2. Mobilization of chloroethene compounds from the rock matrix,” *Groundwater*, vol. 56, no. 2, pp. 317–336, 2018.

[9] M. He and P. Li, “Initial assessment on hydraulic conductivity of rock mass and its size effect using drilling data,” *Groundwater*, vol. 60, no. 6, pp. 820–836, 2022.

[10] K. Baluch, S. Q. Baluch, H.-S. Yang, J.-G. Kim, J.-G. Kim, and S. Qaisrani, “Non-dispersive anti-washout grout design based on geotechnical experimentation for application in subsidence-

prone underwater karstic formations," *Materials*, vol. 14, no. 7, Article ID 1587, 2021.

[11] K. Kirikçi, D. C. Deeming, and A. Gunlu, "Effects of egg mass and percentage mass loss during incubation on hatchability of eggs of the rock partridge (Alectoris graeca)," *British Poultry Science*, vol. 45, no. 3, pp. 380–384, 2004.

[12] B. Pan, X. Wang, Z. Xu, L. Guo, and X. Wang, "Experimental and numerical study of fracture behavior of rock-like material specimens with single pre-set joint under dynamic loading," *Materials*, vol. 14, no. 10, Article ID 2690, 2021.

[13] S. Dong, H. Zhang, Y. Peng, Z. Lu, and W. Hou, "Method of calculating shear strength of rock mass joint surface considering cyclic shear degradation," *Scientific Reports*, vol. 12, no. 1, Article ID 9406, 2022.

[14] M. Nanishi, V. G. Press, J. B. Miller et al., "Hospital-initiated care bundle, posthospitalization care, and outcomes in adults with asthma exacerbation," *The Journal of Allergy and Clinical Immunology: In Practice*, vol. 9, no. 11, pp. 4007–4013.E8, 2021.

[15] J. M. Hartinger, P. Lukáč, P. Mitáš et al., "Vancomycin-releasing cross-linked collagen sponges as wound dressings," *Bosnian Journal of Basic Medical Sciences*, vol. 21, no. 1, pp. 61–70, 2021.

[16] J. Jonak, R. Karpiński, and A. Wójcik, "Influence of the undercut anchor head angle on the propagation of the failure zone of the rock medium," *Materials*, vol. 14, no. 9, Article ID 2371, 2021.

[17] X. Cheng, Y. Ren, X. Du, and Y. Zhang, "Seismic stability of subsea tunnels subjected to seepage," *The Scientific World Journal*, vol. 2014, Article ID 631925, 8 pages, 2014.

[18] B. Khan, S. M. Jamil, T. H. Jafri, and K. Akhtar, "Effects of different empirical tunnel design approaches on rock mass behaviour during tunnel widening," *Heliyon*, vol. 5, no. 12, Article ID e02944, 2019.

[19] J. Zhang, Y. Liu, N. Zhou, and M. Li, "Pore pressure evolution and mass loss of broken gangue during the seepage," *Royal Society Open Science*, vol. 5, no. 10, Article ID 180307, 2018.

[20] L. M. Vandamme and J.-C. Roegiers, "Poroelasticity in hydraulic fracturing simulators," *Journal of Petroleum Technology*, vol. 42, no. 9, pp. 1199–1203, 1990.

[21] B. Liu, J. Li, Q. Liu, and X. Liu, "Analysis of damage and permeability evolution for mudstone material under coupled stress–seepage," *Materials*, vol. 13, no. 17, Article ID 3755, 2020.

[22] J. Liu, L. Zhang, Y. Wei, and Z. Wu, "Coupling model of stress–damage–seepage and its application to static blasting technology in coal mine," *ACS Omega*, vol. 6, no. 50, pp. 34920–34930, 2021.

[23] C. B. Haukwa, Y. W. Tsang, Y.-S. Wu, and G. S. Bodvarsson, "Effect of heterogeneity in fracture permeability on the potential for liquid seepage into a heated emplacement drift of the potential repository," *Journal of Contaminant Hydrology*, vol. 62-63, pp. 509–527, 2003.

[24] J.-S. Pan, S.-X. Yuan, T. Jiang, and C.-H. Cui, "Experimental study on crack characteristics and acoustic emission characteristics in rock-like material with pre-existing cracks," *Scientific Reports*, vol. 11, no. 1, Article ID 23790, 2021.

[25] S. Zhang, W. Qiao, Y. Wu, Z. Fan, and L. Zhang, "Multi-response optimization of ultrafine cement-based slurry using the Taguchi–grey relational analysis method," *Materials*, vol. 14, no. 1, Article ID 117, 2021.

[26] G. S. Esterhuizen, D. F. Gearhart, and I. B. Tulu, "Analysis of monitored ground support and rock mass response in a longwall tailgate entry," *International Journal of Mining Science and Technology*, vol. 28, no. 1, pp. 43–51, 2018.

[27] M. Pang, T. Zhang, Y. Guo, and L. Zhang, "Re-crushing process and non-Darcian seepage characteristics of broken coal medium in coal mine water inrush," *Scientific Reports*, vol. 11, no. 1, Article ID 11380, 2021.

[28] J. Shao, W. Zhang, X. Wu, Y. Lei, and X. Wu, "Rock damage model coupled stress–seepage and its application in water inrush from faults in coal mines," *ACS Omega*, vol. 7, no. 16, pp. 13604–13614, 2022.

[29] B. Hollowoa, L. W. Lamps, J. S. Mizell et al., "Dedifferentiated liposarcoma mimicking a primary colon mass," *International Journal of Surgical Pathology*, vol. 26, no. 2, pp. 174–179, 2018.